Journal of Coordination Chemistry

ISSN: 0095-8972 (Print) 1029-0389 (Online) Journal homepage: http://www.tandfonline.com/loi/gcoo20

Surface-enhanced Raman scattering, electron paramagnetic resonance, and electrochemical activity of copper(II) l-methionine complex/silver nanoparticles/graphene-coupled nanoaggregates

Zhao-Chun Zhang, Hui-Yi Jiang & Zhen-Wei Yu

To cite this article: Zhao-Chun Zhang, Hui-Yi Jiang & Zhen-Wei Yu (2015) Surface-enhanced Raman scattering, electron paramagnetic resonance, and electrochemical activity of copper(II) l-methionine complex/silver nanoparticles/graphene-coupled nanoaggregates, Journal of Coordination Chemistry, 68:1, 18-26, DOI: 10.1080/00958972.2014.985665

To link to this article: http://dx.doi.org/10.1080/00958972.2014.985665

Published online: 04 Dec 2014.

Journal of Coordination Chemistry, 2015
Vol. 68, No. 1, 18–26, http://dx.doi.org/10.1080/00958972.2014.985665

Surface-enhanced Raman scattering, electron paramagnetic resonance, and electrochemical activity of copper(II) L-methionine complex/silver nanoparticles/graphene-coupled nanoaggregates

ZHAO-CHUN ZHANG*, HUI-YI JIANG and ZHEN-WEI YU

Department of Electronic Information Materials, School of Materials Science and Engineering, Shanghai University, Shanghai, China

(*Received 23 July 2014; accepted 8 October 2014*)

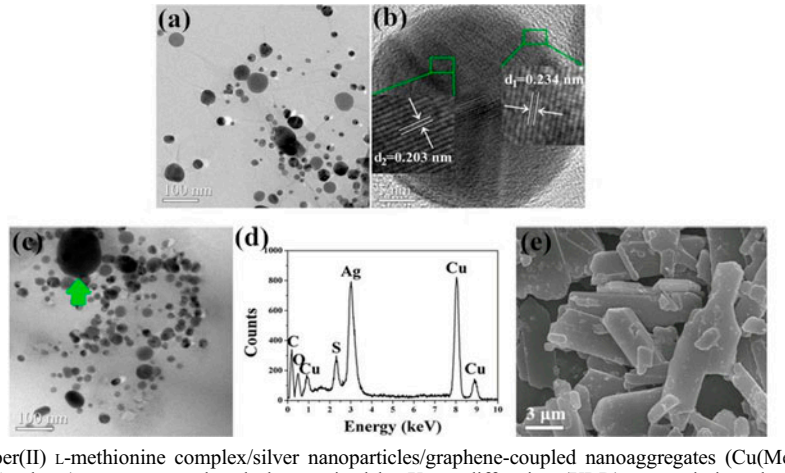

Copper(II) L-methionine complex/silver nanoparticles/graphene-coupled nanoaggregates ($Cu(Met)_2$/Ag/Graphene) were prepared and characterized by X-ray diffraction (XRD), transmission electron microscopy (TEM), Fourier transform infrared spectroscopy (FT-IR), and Raman scattering spectroscopy. Analysis of surface-enhanced Raman scattering of as-prepared nanoaggregate revealed that Cu $(Met)_2$ molecular plane exhibited a perpendicular orientation with respect to the surface of silver nanoparticles. The electrochemical performance of $Cu(Met)_2$/Ag/Graphene investigated by cyclic voltammetry displayed that the redox currents of $Cu(Met)_2$ were enhanced in the presence of Ag/Graphene. The electron paramagnetic resonance spectrum performed at room temperature showed that compared with $Cu(Met)_2$ powder the *g* value of $Cu(Met)_2$/Ag/Graphene reduced slightly, indicating minor discrepancies of the local magnetic field around the copper ions between $Cu(Met)_2$ powder and $Cu(Met)_2$/Ag/Graphene coupled nanoaggregates.

Keywords: Copper(II) L-methionine complex; Graphene; Silver; Nanoaggregate; Surface-enhanced Raman scattering; Electrochemistry

*Corresponding author. Email: zhangzhaochun@shu.edu.cn

1. Introduction

Because of unique nanostructure and extraordinary properties, graphene is a promising nanoscale building block of new nanocomposites [1]. Graphene has been utilized as support to disperse and stabilize noble metal nanoparticles (e.g., Au, Pt, Pd). The structural complexity at graphene/metal nanoscale interfaces holds much promise for manifestation of emergent phenomena and provides a means to modulate the electronic structure of graphene [2]. Cu(II)–methionine complex has showed some antiulcer activity as revealed by animal model studies and has also found some interest in veterinary medicine, for copper supplementation [3]. A strategy for extending the potential application of Cu(II) complexes is to construct nanocomposite materials with graphene. These nanocomposite materials could bring new properties which may be greatly changed from starting material [4].

The work reported herein is focused on the preparation of nanoaggregates of copper(II)–methionine complex with silver nanoparticles/graphene. Surface-enhanced Raman spectroscopy, electron spin resonance, and electrochemical activity have been studied. It is hoped that such study will give further insight into the type of Cu(II) amino acid complexes with distinct morphology and properties.

2. Experimental

2.1. *Synthesis of copper(II) L-methionine complex by chemical coprecipitation*

In 20 mL of water, 2.416 g of $Cu(NO_3)_2 \cdot 3H_2O$ was dissolved. In 50 mL of water, 2.984 g of L-methionine was dissolved and 3.25 mL of NaOH (30%) was added for deprotonation of the amino acid. The $Cu(NO_3)_2$ aqueous solution was added to the deprotonated amino acid solution and the mixture was stirred for 1 h. The gray-blue precipitate was filtered off and washed with water. The precipitate was then dried in air at 40 °C for 6 h.

2.2. *Preparation of Ag/Graphene nanoaggregates by liquid-phase reducing method*

Graphite oxide was prepared from spectrum pure graphite powder via the modified Hummers method. Graphene oxide suspension was obtained by dispersing graphite oxide powder in deionized water with the aid of sonication in an ultrasonic bath cleaner (100 W, 40 kHz). In a typical procedure, a homogeneous yellow–brown dispersion with a concentration of about 0.67 mg mL^{-1} was obtained by 3 h of sonication. Analysis of the AFM topographic images revealed graphene sheets with lateral dimensions of 2–8 μm and with an average thickness of ~3.5 nm [5].

In a 50-mL conical flask, 100-mL, 0.67 mg mL^{-1} graphene oxide aqueous dispersion was placed. To this, a solution of 369 mg $AgNO_3$ in 20 mL of water was added. In dark conditions, the mixture was stirred for 12 h. To the mixture so formed, 0.22-mL, 50% $N_2H_4 \cdot H_2O$ in 10 mL of water was slowly added. After about 30 min, the mixture was centrifuged and washed with distilled water three times to remove the remaining reagents. The dark product was then dried in air at 40 °C for 4 h.

2.3. *Preparation of Cu(Met)$_2$/Ag/Graphene nanoaggregates by heterogeneous nucleation and growth method*

In 50 mL of water, 150 mg of Ag/Graphene and 2.984 g of L-methionine were dispersed with vigorous stirring for 2 h and 30% NaOH aqueous solution was slowly added into the mixture until the pH was 7. To this, 2.416 g of $Cu(NO_3)_2 \cdot 3H_2O$ in 20 mL water was slowly added with continuous stirring for 2 h and then allowed to stand for 2 h. The precipitated Cu(Met)$_2$/Ag/Graphene powder was filtered off and rinsed several times with water, followed by drying in air at 40 °C for 8 h.

2.4. *Characterization and measurement*

X-ray powder diffraction (XRD, $\lambda = 1.5418$ Å) was collected at 2θ scanning rate of 4° min^{-1} on a Rigaku D/MAX-RC. Morphological characterizations were performed by transmission electron microscopy (TEM, JEM-2010) and energy dispersive spectrum (EDS), operated at 200 kV. The quantitative result of Cu(Met)$_2$/Ag/Graphene was displayed by X-ray fluorescence (XRF, XRF-1800, Shimadzu Limited). The Raman spectra were conducted by using a Renishaw InVia plus spectrometer equipped with an Ar^+ ion laser. Powder EPR measurements were performed at room temperature at 9.4 GHz (X band) using standard JEOL-JES-FA200 equipment.

Cyclic voltammetry (CV) measurements were carried out with a standard three-electrode (glassy carbon electrode (GCE), platinum wire and saturated Hg/Hg_2Cl_2 (SCE)) cell using a 12558WB electrochemical Workstation (Solartron, Britain). In 2.0 mL of ethanol, 5 mg of the sample was well dispersed by ultrasonic dispersion. To this dispersion, 50 µl of Nafion was added. Onto the glassy-carbon disk, 10 µl of the ethanol dispersion was then dropped. The measurement was carried out at room temperature for the cyclic voltammetry at 25 mV s^{-1} for the scan in 0.1 M KCl electrolyte solution.

3. Results and discussion

3.1. *XRD analysis*

Cu(Met)$_2$/Ag/Graphene aggregates were prepared from copper(II)–L-methionine complex and Ag/Graphene. The high crystallinity of both copper(II)–L-methionine complex and Ag was evident from the XRD pattern of the as-prepared sample, as shown in figure 1. Comparative analysis revealed that four diffraction peaks consistent with the (1 1 1), (2 0 0), (2 2 0), and (3 1 1) crystalline planes of face-centered cubic (fcc) Ag appeared and the corresponding *d*-spacing values were 0.234, 0.203, 0.145, and 0.123 nm, respectively. Compared with the high intensity of diffraction peaks of Ag nanoparticles, the diffraction peaks with smaller intensities were indexed for the Cu(Met)$_2$. It could also be noticed that the (0 0 2) diffraction peak of the reduced graphene oxide was not observed.

Structural data reported elsewhere [6] show that Cu(Met)$_2$ crystallizes in the $P2_1$ space group with two molecules per unit cell. Trans coordination of two methionine molecules per Cu(II) generates an equatorial N_2O_2 ligand set. Additional interaction with two carboxylate oxygens from neighboring methionine molecules brings about the apical bonds and links the Cu(II) species into a carboxylate-bridged sheet structure. The copper ions in

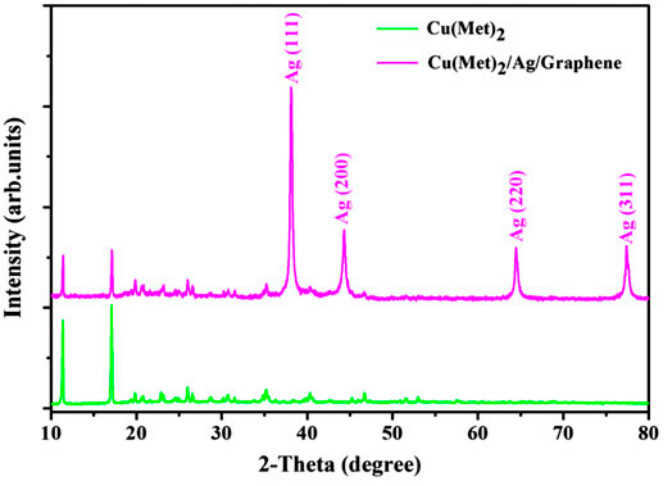

Figure 1. X-ray diffraction patterns of $Cu(Met)_2$/Ag/Graphene compared with $Cu(Met)_2$.

both complexes are in isolated sheets perpendicular to crystal axis *c*. The ions within a layer are bridged through the carboxylate oxygens which occupy the apical sites in the copper coordination spheres.

3.2. *Morphology characterizations*

Figure 2(a) presents the TEM image of Ag/Graphene samples. A plicated sheet-like graphene coupled with subrotund silver nanoparticles with the equivalent diameter in the range of 10–50 nm were observed, indicating construction of Ag/Graphene nanoaggregates. The thickness of graphene was measured to be about 3.5 nm [5], larger than the value of 0.8 nm referred for a single-layer graphene [7, 8]. Figure 2(b) presents the lattice fringe image of a silver nanoparticle. Parallel fringes with the space of 0.234 nm (d_1) and 0.203 nm (d_2) are consistent with the space of (1 1 1) and (2 0 0) lattice planes of face-centered cubic Ag.

The existence of $Cu(Met)_2$ complexes on Ag/Graphene was assessed as shown in figure 2(c). The oval $Cu(Met)_2$ particle larger than Ag particles was observed. The long axis of the $Cu(Met)_2$ particle is about 120 nm. Figure 2(d) shows the EDS spectrum from the specific region [arrow, figure 2(c)] of the $Cu(Met)_2$/Ag/Graphene nano-aggregation. In the EDS spectrum, two distinct peaks of Ag and Cu, and also the presence of C, O, and S peaks were observed. In order to quantitatively confirm the presence of $Cu(Met)_2$ complexes, the $Cu(Met)_2$/Ag/Graphene nanoaggregation was used simultaneously for X-ray fluorescence measurement. The XRF result showed that the mass percentages of C, Ag, O, S, and Cu elements were 51.28, 16.66, 13.64, 10.06, and 8.36%, respectively.

Figure 2(e) presents a typical SEM image of the copper–methionine complex sample prepared by chemical coprecipitation. A mass of plates appeared to be stacked randomly. Most plates had narrow irregular polygon geometric features with an equivalence diameter of micron order of magnitude.

Comparison and analysis of the morphologies shown in figures 2(c) and (e) reflect that the microstructures of copper–methionine complex prepared by homogenous nucleation and heterogeneous nucleation are different. In the presence of Ag/Graphene nanoaggregates, the

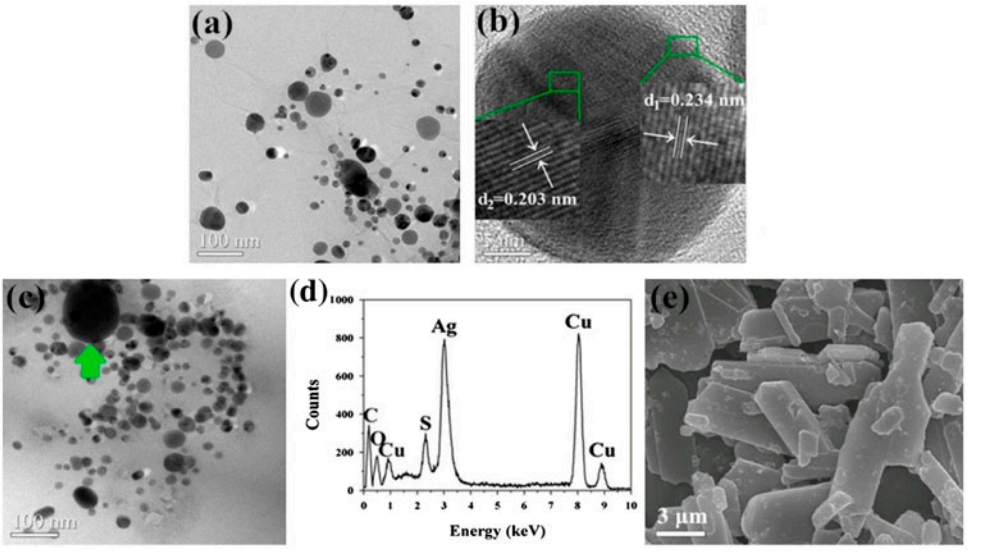

Figure 2. (a) TEM image of Ag/Graphene, (b) HRTEM image of Ag nanoparticles, (c) TEM image of $Cu(Met)_2$/Ag/Graphene, (d) EDS spectrum of $Cu(Met)_2$/Ag/Graphene (arrow) in (c), and (e) SEM image of $Cu(Met)_2$.

nucleation and growth of copper–methionine complex crystal might take priority in silver nanoparticles in view of the affinity between silver and nitrogen, oxygen, or sulfur.

3.3. *Vibrational spectra analyses*

For typical absorption bands, the IR spectrum of $Cu(Met)_2$/Ag/Graphene nanoaggregates is roughly identical to that of $Cu(Met)_2$ powder, as shown in figure 3. The low transmittance of $Cu(Met)_2$/Ag/Graphene nanoaggregates reflected the characteristics of infrared adsorption of graphene. The bands at 3450, 1620, 1703, and 1219 cm^{-1} are assigned to O–H stretching, C=C stretching, C=O stretching from carboxylic groups, and C–OH stretching vibrations [6], respectively. The bands at 2851 and 2920 cm^{-1} are due to symmetric and antisymmetric CH_2 stretches, respectively. Two sharp bands at 3299 and 3242 are assigned to $–NH_2$ stretching vibrations. The bands at 448.2 and 414.02 cm^{-1} are contributed by Cu–N and Cu–O stretches [3], respectively.

Figure 4 shows the Raman scattering spectra of $Cu(Met)_2$ powder and $Cu(Met)_2$/Ag/Graphene nanoaggregates. The main features of the Raman spectrum for $Cu(Met)_2$/Ag/Graphene nanoaggregates are the D band at 1332 cm^{-1} due to the breathing modes of sp^2 atoms in rings, and G band at 1593 cm^{-1} due to the bond stretching of all pairs of sp^2 atoms in both rings and chains for laser excitation at 3.14 eV [9]. The 2-D band around 2649 cm^{-1} and D + G band around 2913 cm^{-1} are also observed. The 2-D peak in graphene is due to two phonons with opposite momentum in the highest optical branch near the *K* point of the Brillouin zone [9]. However, the signal-to-noise of the present Raman spectrum is not able to support us to analyze the disorder of graphene in the $Cu(Met)_2$/Ag/Graphene nanoaggregates.

The Raman spectrum of $Cu(Met)_2$/Ag/Graphene nanoaggregates exhibits two intense peaks of $Cu(Met)_2$ at 517 and 595 cm^{-1} due to the in plane Cu–N stretching and O=C–O

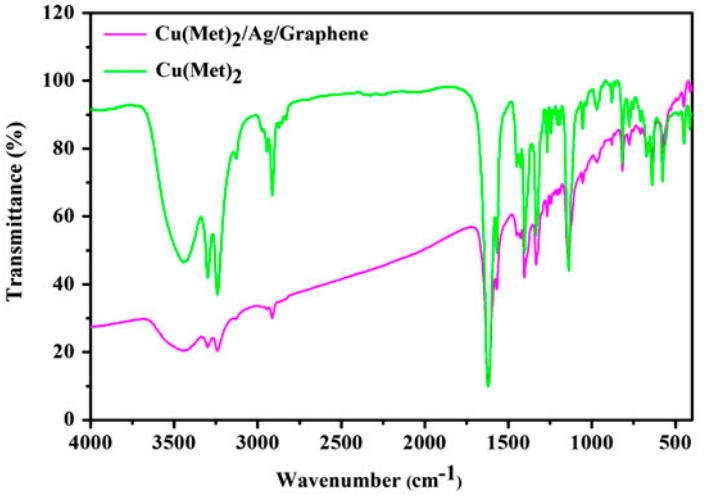

Figure 3. FT-IR spectra of $Cu(Met)_2$ and $Cu(Met)_2$/Ag/Graphene.

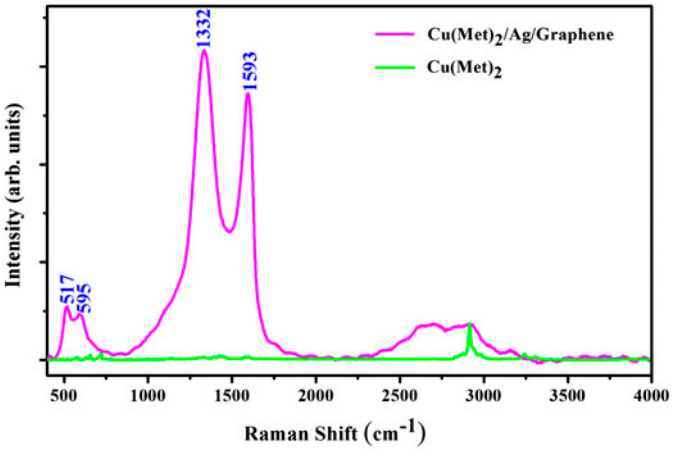

Figure 4. Raman spectra of $Cu(Met)_2$ and $Cu(Met)_2$/Ag/Graphene.

bending vibrations, respectively. In comparison with other Raman peaks of $Cu(Met)_2$, there is an abrupt increase in the Raman scattering intensities of the two bands when the complex precipitates on Ag/Graphene nanoaggregates; intensity enhancement of the two bands is observed. It has been demonstrated that nanosheets combined with Ag nanoparticles have SERS activity via electromagnetic (EM) field enhancement of the Ag nanoparticles and charge-transfer (CT) between the energy levels of the molecule and Fermi levels of the Ag nanoparticles [10]. Here, the mechanisms for this enhancement can be attributed largely to the EM fields of the Ag nanoparticles associated with large local fields caused by surface plasmon (SP). Coupled SP plays an important role of EM hot spots owing to the aggregation of Ag nanoparticles that have intense local EM fields, leading to strong Raman enhanced signals. Moreover, the interaction between Ag nanoparticles and graphene may

bring about the formation of CT complexes, which augment the chemical enhancement of SERS on Ag/Graphene nanoaggregates.

The enhancement of different vibrational modes is usually dependent on the geometry of the molecules on the surface of silver nanoparticles. There are three main configurations that can be adopted: end-on, edge-on or flat. On the basis of the surface selection rules, the intensity enhancement of Cu–N stretching mode first rules out the possibility of the orientation involving the molecules lying parallel to the silver surface.

The end-on linkage would require an attachment through one sulfur. One might argue that such an attachment is possible because of the affinity of silver and sulfur. However, no significant change in the C–S stretching mode, 775 cm^{-1} [11], is observed. The changes in the observed intensities of the Cu–N stretching and O=C–O bending modes could not be accounted for by this configuration. In fact, unlike alkanethiols and dialkyl disulfides, the dialkyl sulfide molecules possess fairly weak bonding interactions with silver.

The edge-on linkage would require an attachment through one amino nitrogen or carboxylic oxygen. The large increases in the observed intensities of the Cu–N stretching and O=C–O bending modes could be accounted for by this configuration. This mode would be perpendicular to the silver surface, making it suited for enhancement via the electromagnetic effect. It would also be pointed out that an edge-on attachment should be reflected in some changes in the COO^- symmetrical stretching mode, 1408 cm^{-1}, and asymmetrical stretching mode, 1584 cm^{-1} [11]. It is very difficult, however, to observe the increases in the COO^- stretching mode because of the overlapping of the D mode at 1332 cm^{-1} and G mode at 1593 cm^{-1} of graphene.

3.4. *Electron paramagnetic resonance*

Powder EPR spectra (figure 5) at room temperature are typical for monomeric species with square planar local symmetry around the metal ion. The principal values of the *g*-factor of $Cu(Met)_2$ and $Cu(Met)_2$/Ag/Graphene are 2.0930 and 2.0412, respectively, indicating the

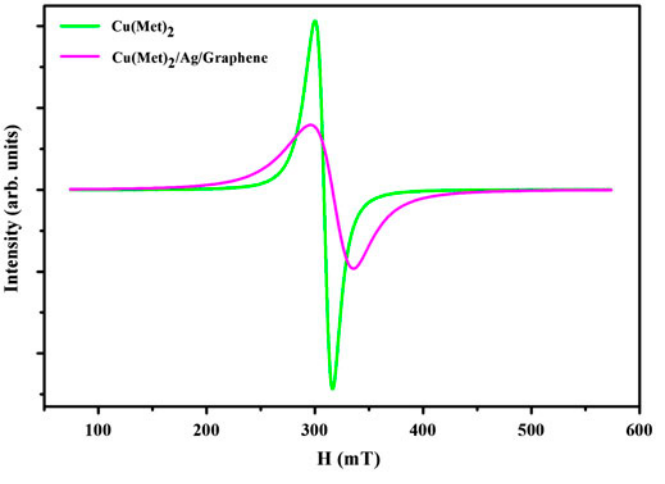

Figure 5. EPR spectra of $Cu(Met)_2$ and $Cu(Met)_2$/Ag/Graphene at room temperature.

presence of an unpaired electron in a $d_{x^2-y^2}$ orbital. From the comparison of two values, the g value of $Cu(Met)_2$/Ag/Graphene is slightly smaller than that of $Cu(Met)_2$.

The g-factor, the resonant position of EPR, is given by: $g = h\nu_0/\beta H_r$, and is therefore dependent upon the local magnetic field strength, H_r, under the same test conditions. It is obvious that the decrease of g-factor requires increase in the local magnetic field strength. Such an increase might be possible because of the presence of Ag/Graphene nanoaggregates. Although the fundamental basis of the enhancement of local magnetic field for this system has yet to be fully understood, it is believed that the effect of Ag/Graphene nanoaggregates on the local magnetic field played a role in investigating the electron paramagnetic resonance for $Cu(Met)_2$/Ag/Graphene-coupled nanoaggregates.

3.5. *Electrochemical activity*

The CV of the $Cu(Met)_2$ and $Cu(Met)_2$/Ag/Graphene-modified GCE in 0.1 M KCl are shown in figure 6. The $Cu(Met)_2$ powder showed peaks at −0.07 V (A1) and 0.18 V (A2) during the anodic cycle. The peak at −0.07 V was attributed to oxidation of Cu(0) to Cu(I). The peak at 0.18 V was attributed to the combination of two processes: the oxidation of Cu (I) to Cu(II) and also oxidation of Cu(0) to Cu(II) [12]. The oxidation processes can be expressed as the following reactions:

$$\text{A1} : \text{Cu} + \text{Cl}^- - \text{e}^- \rightarrow \text{CuCl}$$

$$\text{A2} : \text{CuCl} - \text{e}^- \rightarrow \text{Cu}^{2+} + \text{Cl}^- \quad \text{Cu} - 2\text{e}^- \rightarrow \text{Cu}^{2+}$$

During the cathodic cycle, the peak at 0.08 V (C1) was attributed to the combination of two processes: the reduction of Cu(II) to Cu(I) and also reduction of Cu(II) to Cu(0). The peak at −0.6 V (C2) was attributed to the reductions of Cu(I) to Cu(0).

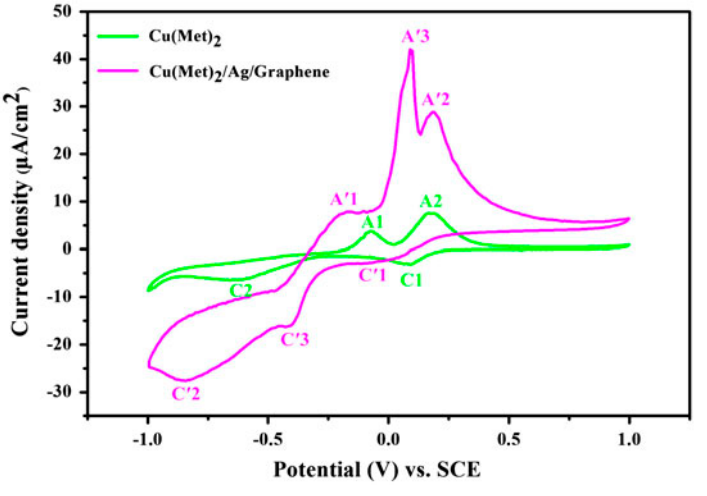

Figure 6. Cyclic voltammograms of $Cu(Met)_2$ and $Cu(Met)_2$/Ag/Graphene in 0.1 M KCl at scan rate of 25 mV s^{-1}.

For the $Cu(Met)_2$/Ag/Graphene nanoaggregates, four peaks at −0.17 V (A′1) and 0.18 V (A′2) during the anodic cycle and −0.06 V (C′1) and −0.86 V (C′2) during the cathodic cycle were attributed to electrooxidation and electroreduction of copper element. These half-reactions are the same as those of $Cu(Met)_2$ powder. However, a high oxidation peak at 0.1 V (A′3) was probably caused by oxidation of Ag(0) to Ag(I) and a reduction peak at −0.17 V (C′3) by the reduction of Ag(I) to Ag(0), described by the following reactions:

$$A'3 : Ag + Cl^- - e^- \rightarrow AgCl$$

$$C'3 : AgCl + e^- \rightarrow Ag + Cl^-$$

It is clear from figure 6 that the peak currents of A′1, A′2, and C′2 are larger than that of A1, A2, and C2, indicating a high electrical conductivity and fast electron transfer at the electrode surface modified by $Cu(Met)_2$/Ag/Graphene with respect to that by $Cu(Met)_2$. Taking into consideration the same amount of $Cu(Met)_2$ and $Cu(Met)_2$/Ag/Graphene on the modified glassy carbon electrode, it can be concluded that the electrochemical activity of $Cu(Met)_2$ is enhanced by the coupled Ag/Graphene nanoaggregates, although the enhancement mechanism is still unclear.

4. Conclusion

By wet chemistry technique, oval $Cu(Met)_2$ particles were synthesized on the surface of Ag/Graphene. On the basis of the surface selection rules and SERS Raman data, it can be inferred that the $Cu(Met)_2$ molecules adopt edge-on linkage configuration on the Ag surface. The cyclic voltammograms show that $Cu(Met)_2$/Ag/Graphene-coupled nanoaggregates possess enhanced electrochemical activity compared to $Cu(Met)_2$.

References

[1] D. Li, R.B. Kaner. *Science*, **320**, 1170 (2008).
[2] B.J. Schultz, R.V. Dennis, V. Lee, S. Banerjee. *Nanoscale*, **6**, 3444 (2014).
[3] C.C. Wagner, E.J. Baran. *Acta Farm. Bonaerense*, **21**, 287 (2002).
[4] J.-P. Andreassen. *J. Cryst. Growth*, **274**, 256 (2005).
[5] H. Zheng, S. Yang, J. Zhao, Z. Zhang. *Appl. Phys. A*, **114**, 801 (2014).
[6] C.-C. Ou, D.A. Powers, J.A. Thich, T.R. Felthouse, D.N. Hendrickson, J.A. Potenza, H.J. Schugar. *Inorg. Chem.*, **17**, 34 (1978).
[7] K.S. Novoselov, A.K. Geim, S.V. Morozov, D. Jiang, Y. Zhang, S.V. Dubonos, I.V. Grigorieva, A.A. Firsov. *Science*, **306**, 666 (2004).
[8] A. Gupta, G. Chen, P. Joshi, S. Tadigadapa, P.C. Eklund. *Nano Lett.*, **6**, 2667 (2006).
[9] A.C. Ferrari. *Solid State Commun.*, **143**, 47 (2007).
[10] Q. Zhou, X.W. Li, Q. Fan, X.X. Zhang, J.W. Zheng. *Angew. Chem. Int. Ed.*, **45**, 3970 (2006).
[11] B. Onoa, V. Moreno. *Trans. Met. Chem.*, **23**, 485 (1998).
[12] W.Z. Teo, A. Ambrosi, M. Pumera. *Electrochem. Commun.*, **28**, 51 (2013).